UCRL-JC-124925
PREPRINT

Modeling of Filamentation Damage Induced in Silica by 351-nm Laser Pulses

D. Milam
J. T. Hunt
K. R. Manes
W. H. Williams

This paper was prepared for submittal to the
Symposium on Optical Materials for High Power Lasers '96
Boulder, CO
October 7-9, 1996

October 17, 1996

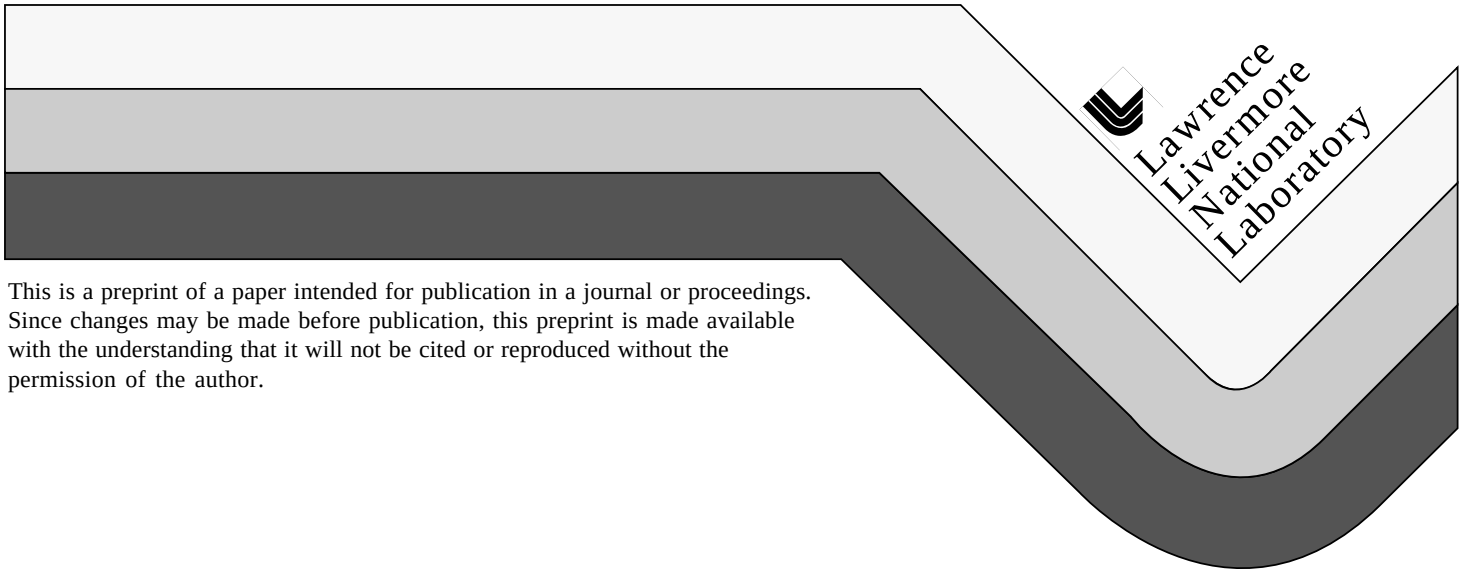

Modeling of filamentation damage induced in silica by 351-nm laser pulses

D. Milam, J. T. Hunt, K. R. Manes and W. H. Williams
Lawrence Livermore National Laboratory
Livermore, California, 94550

ABSTRACT

A major risk factor that must be considered in design of the National Ignition Facility is the possibility for catastrophic self-focusing of the 351-nm beam in the silica optical components that are in the final section of the laser. Proposed designs for the laser are analyzed by the beam-propagation code PROP92. A 351-nm self-focusing experiment, induction of tracking damage, was done to provide data for validation of this code. The measured self-focusing lengths were correctly predicted by the code.
Key words: self-focusing, silica, 351-nm, intensity-length product

1. INTRODUCTION.

Proposed laser designs for the National Ignition Facility[1] are analyzed by a recently developed code, PROP92, which can treat one or two transverse dimensions and one linear polarization[2]. The code uses fast-Fourier-transform propagators on a rectangular grid. It models amplification, losses, refraction, diffraction and harmonic conversion.

The codes must also describe the modification by small-scale self-focusing of the intensity distribution in the beam. Modeling of self-focusing begins with decomposition of the input laser beam into a distribution of plane waves. The spatially averaged intensity can be attributed to a primary component with amplitude $\mathbf{E}_p$ and propagation vector $\mathbf{k}_p$. Ripple on the input beam can be attributed to interference between the primary field ($\mathbf{E}_p$, $\mathbf{k}_p$) and a family of weak secondary fields ($\mathbf{E}_\theta$, $\mathbf{k}_\theta$), where θ is the angle between $\mathbf{k}_\theta$ and $\mathbf{k}_p$.

Propagation of this input field through a laser chain causes amplification of the amplitudes $\mathbf{E}_\theta$ of the noise waves, and therefore, increase in the depth of the intensity ripple. There is an intuitive model that describes this amplification as scattering from an induced refractive-index grating. The refractive index is usually written as $n = n_o + \gamma I$, where the coefficient γ gives the induced change in index per unit intensity, I. When one of the weak fields is superimposed onto the primary beam, the intensity variation in the optical interference pattern causes an induced periodic change of index in the glass through which the pulse is propagating. Reflection from the induced grating moves an equal fraction of the energy in each of the two interfering waves into the other; the net flow of energy is from the intense primary wave into the weak wave.

Analysis by Bespalov and Talanov[3] indicated preferential amplification for weak waves that were propagating at angles within a band $\Delta\theta$ centered at $\theta_m = \sqrt{2\gamma I}$. For fused silica, $\gamma = 2.7 \times 10^{-16}$ cm^2/W at 1053 nm[4], and θ_m ranges from 1300 μrad at intensity of 3 GW/cm^2 to 1600 μrad at 5 Gw/cm^2. For these angles, the characteristic ripple dimensions are $\Delta x = \lambda/\theta = 0.6$ to 0.8 mm.

Several tests have been done to confirm that the code PROP92 accurately describes nonlinear refraction of a 1053-nm beam during its propagation through a Nd:glass laser[5]. At the output of our fusion lasers, the 1053-nm beam is harmonically converted to 351 nm. The 351-nm beam propagates through a few silica components to the fusion target. This paper describes modeling of a small-scale 351-nm self-focusing experiment that was done to verify that PROP92 adequately describes nonlinear refraction of this ultraviolet beam.

2. EXPERIMENTAL ARRANGEMENT

A diagram of the experiment is shown in Fig. 1. The 351-nm beam was generated by harmonic conversion of a 1053-nm beam. The arrangement of the experiment was selected to allow (1) separation of the residual 1053- and 527-nm light, (2) preservation of the optimal intensity distribution in the 351-nm beam, and (3) careful disgnostics for the 351-nm light.

The 1053-nm source laser provided 1-ns pulses in a 22-mm-diameter beam that had been shaped by apodization and image relaying. In such a laser, the 1053-nm beam intensity is most uniform in image-relay planes, and the 351-nm beam with optimal uniformity is obtained by placing the convertor

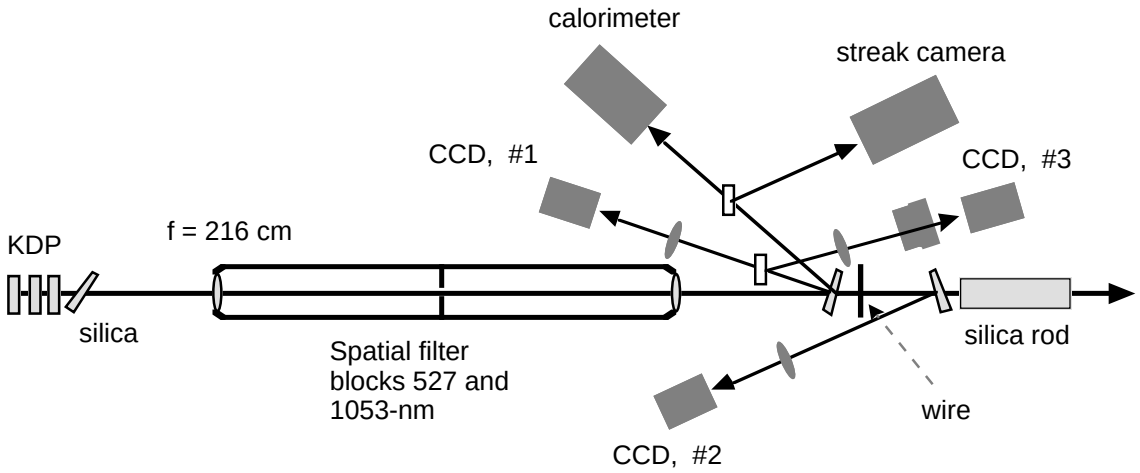

Fig. 1. Experimental arrangement. Cameras #1, #2--fluence distributions at plane of wire and at input plane to the sample. Camera #3--Alignment of pinhole.

crystals in such a plane. As either the 351-nm or the 1053-nm beam propagates away from an image-relay plane, the uniformity of its intensity degrades. Therefore, 351-nm experiments should be conducted in the immediate proximity of the KDP crystals. This requirement complicates frequency separation.

Circumvention of the principal difficulties was done by incorporating an image-relaying spatial filter into our experiment. The multi-frequency beam from the convertor was passed through a 3^o silica prism and a spatial filter. The pinhole in the filter was positioned to transmit the 351-nm light; it blocked the residual 527- and 1053-nm beams. The lenses in the filter also served as an image-relay pair. They imaged the exit plane of the KDP crystals onto a plane in the center of the self-focusing sample. The angular acceptance angle of the spatial filter was 250 μrad (half angle). Therefore, relay-imaging of the 351-nm beam preserved its optimally uniform intensity, and largely eliminated intensity modulation with characteristic dimension smaller than $\Delta x = 1.4$ mm.

The filtered 351-nm beam propagated through two bare silica splitters and a silica rod with length of 20 cm. During most experiments, a wire was placed in the beam at a distance of 1 m from the sample. The fluence distribution in the 351-nm beam, at the plane of the wire and at the input plane of the sample, was recorded by CCD cameras. Pulse energy was measured with an absorbing-glass calorimeter, and the pulse waveform was recorded by a streak camera.

Because accurate recording of the fluence distribution was a primary objective of the experiment, we initially used redundant CCD cameras. Two cameras were used to record a single plane in the beam. The two diagnostic beams for these cameras were reflected from the opposite sides of a wedged silica splitter. Each diagnostic beam contained a single lens that imaged the selected beam plane onto the camera, and attenuators that were made of absorbing-glass filters. We found that all of our absorbing-glass filters caused significant phase distortion. With propagation, phase error is converted into amplitude error that can be observed by the cameras. Conversion from phase error to amplitude error was largely eliminated by placing the filters either very close to the camera (image plane) or in the object plane. Image distortion by the silica lenses and splitters, and by the CCD cameras, was not a significant problem. At the end of this effort, we had learned to make redundant recordings that contained essentially identical images of large-scale (1-5 mm) intensity ripple, but some differences remained for smaller ripple, which is in fact most important in a 351-nm self-focusing experiment. A typical image of the fluence distribution in the beam is shown in Fig. 2.

Once we had the diagnostics installed, the experiment was particularly simple. The energy was sequentially increased until tracking damage was observed in the sample. The length of the tracked region was determined through visual inspection with intense white-light illumination. The untracked length in front of the damage was defined to be the self-focusing length, L. Note that the thickness of the two silica splitters possibly should be included in L, but this is not required in a test of the codes. The intensity was defined to be the spatial average (over a circular aperture with diameter of 15 mm) at the maximum in the temporal waveform. Table I contains the measured results.

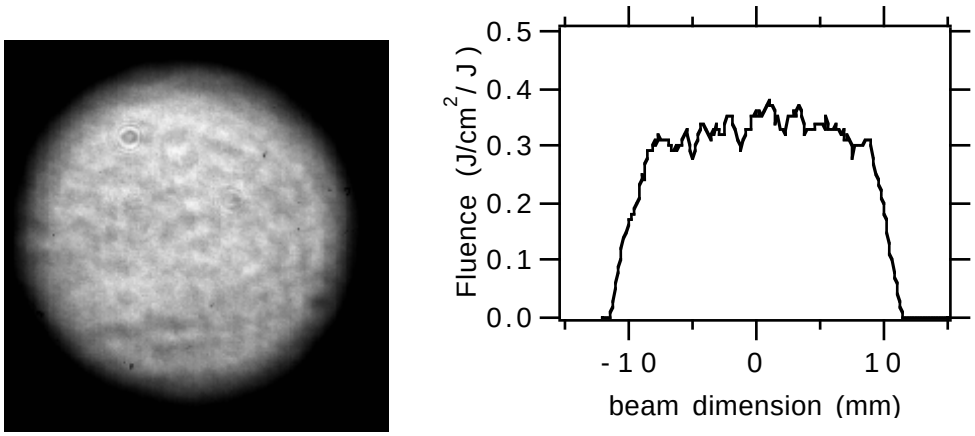

Fig. 2. Fluence distribution in the 351-nm beam. Left: CCD camera image. Right: Horizontal cut through the beam.

Table 1. Measured intensity-length products for filamentation by self-focusing of 351-nm light in fused silica.

Sample	Obscuration	Intensity (GW / cm^2)	Length (cm)	IL Product (GW / cm)
#1	none	2.40 ± 0.16	13.5 ± 0.5	32.4 ± 2.6
#1	wire	1.46 ± 0.11	17.0 ± 0.5	25.0 ± 2.5
#1	wire	1.90 ± 0.13	12.5 ± 0.5	24.0 ± 2.5
#1	wire	1.55 ± 0.10	16.0 ± 0.5	25.0 ± 2.5

3. MODELING

The recorded image of the fluence distribution in the 351-nm beam, in the plane of the wire, was used as input to PROP92. It was placed on a square grid that was just large enough to contain the beam. Usually, the grid contained 1024 x 1024 pixels. We assumed that the nonlinear refractive index coefficient of silica was $(3.6 \pm 0.6) \times 10^{-16}$ cm^2/W at 351 nm[4]. If a wire had been used in the experiment, its shadow was imposed on the beam mathematically. The code then propagated the beam through the splitters and the sample, and for each spatial step along the beam path, recorded the largest intensity anywhere within the beam.

Two examples are shown in Fig. 3. The calculated intensity increased abruptly at a particular position in the rod, and then stabilized at a value that was governed by the pixel size in the grid. That is, an additional increase in the intensity was not observed once the diameter of a self-focusing filament was less than the width of a pixel.

For the case with a wire in the beam, there is close agreement between the position of the steep rise in calculated intensity and the measured tracking length. Without the wire, the agreement is acceptable, but not so precise. We believe that the reduction in precision for the latter case is a result of depending solely on the CCD image for a determination of the input ripple. Finally, it is interesting to note that exact knowledge of the bulk damage threshold is not required because the increase in intensity is so abrupt.

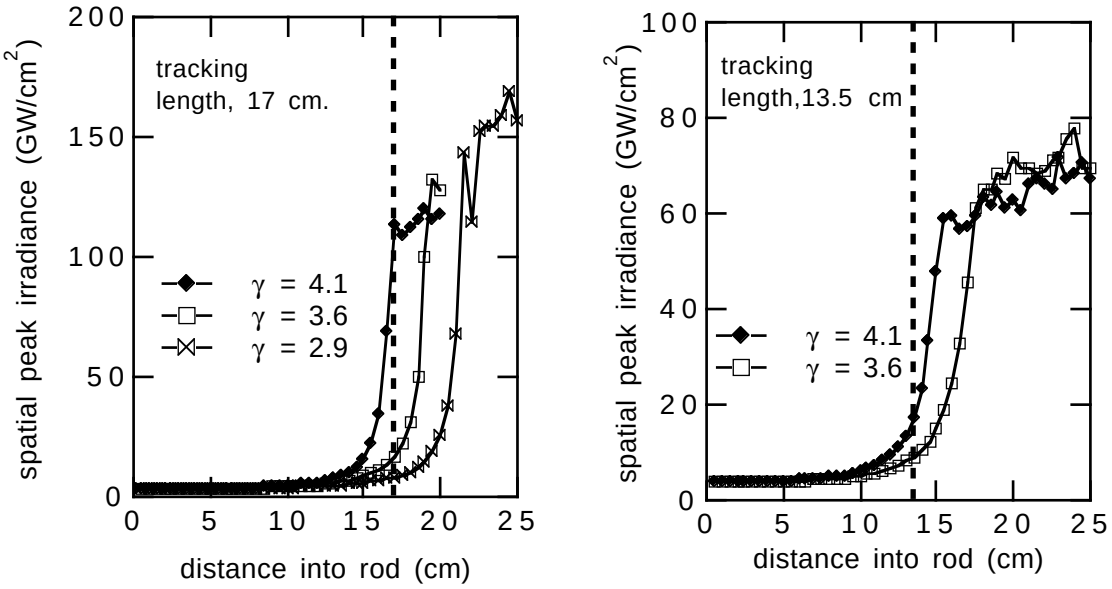

Fig. 3. Calculation of intensity vs propagation distance in the silica sample for three values of the self-focusing coefficient. Tracking damage was observed in the sample in the region beyond the boundary that is indicated by the dashed lines. Left: A wire with diameter of 225 μm was in the beam. Right: No wire.

4. Summary.

We conclude that PROP92 can predict catastrophic self-focusing of a well characterized beam. For a wavelength of 351-nm, the measured intensity-length products were 25-30 GW/cm. These values are based on the length of the undamaged path in the silica sample; the path through the two silica splitters was ignored. We will do additional calculations to determine whether self-focusing in the two silica samples was important. If their thicknesses can be included, the IL products are more favorable, 30-37 GW/cm.

Finally, it is important to note that this experiment was a particularly challenging test of the code, i.e., the prediction of a singularity. It was not a direct measurement of the IL product that should be used in the design of the final optics package for NIF. The measured IL products depended on the induced phase shift, and on both the the strength and scale length of the input ripple. The allowable IL product for NIF will depend partially on the ripple on the NIF beam.

5. Acknowledgements

We are grateful for the assistance of Walter Sell who maintained and operated the laser during these experiments, and collected most of the data. Work was performed under the auspices of the U. S. Department of Energy by Lawrence Livermore National Laboratory under contract No. W-7405-Eng-48.

6. References.

1. J. A. Paisner, J. D. Boyer, S. A. Kumpan, W. H. Lowdermilk and M. S. Sorem, "Conceptual design of the National Ignition Facility," in First Annual International Conference on Solid State Lasers for Application to Inertial Confinement Fusion, M. Andre and H. T. Powell Eds., SPIE vol. 2633, 2-11, 1995.
2. The code PROP92 is a composite of two codes, PROP1 and PROP2. They evolved from earlier codes BTGAIN, ZAX, SNORT, LAMP, ARTEMIS and MALAPROP that were developed at Livermore and are reviewed in W. W. Simmons, J. T. Hunt and W. E. Warren, “Light propagation through large systems, “ IEEE J. Quant. Electron., **QE-17**, 1727-1743, 1981. Liberal use has also been made of the code OASIS that was originally developed by Rockwell Rocketdyne, Inc. under contract with the U. S. Air Force.
3. V. I. Bespalov and V.I. Talanov, “Filamentary structure of light beams in nonlinear liquids,” JETP Lett., **3**, 307-312, 1966.
4. D. Milam, unpublished review of the literature for self-focusing in silica.
5. W. H. Williams, K. R. Manes, J. T. Hunt, P. A. Reynard, D. Milam and D. Eimerl, "Modeling of self-focusing experiments by beam propagation codes," ICF Quarterly Rept., UCRL-LR-105821-96-1